Turbulence modelling and turbulent inlet on a blunt plate

Vita, Giulio; Hemida, Hassan; Baniotopoulos, C

Document Version
Peer reviewed version

Citation for published version (Harvard):
Vita, G, Hemida, H & Baniotopoulos, C 2018, Turbulence modelling and turbulent inlet on a blunt plate: a numerical study. in AL Materazzi & I Venanzi (eds), *Proceedings of the XIV Conference of the Italian Association for Wind Engineering - IN-VENTO 2016.* Morlacchi University Press, XIV Conference of the Italian Association for Wind Engineering, Terni, Italy, 25/09/16.

[Link to publication on Research at Birmingham portal](#)

Turbulence modelling and turbulent inlet on a blunt plate: a numerical study

Giulio Vita, Hassan Hemida and Charalampos Baniotopoulos

Department of Civil Engineering, School of Engineering, University of Birmingham
Birmingham, United Kingdom
Corresponding author: Giulio Vita, g.vita@bham.ac.uk

Abstract

Free Stream Turbulence is usually disregarded as a governing parameter in the assessment of aerodynamic forces. However, an effect is noticeable on the aerodynamic coefficients if turbulence is added at the inlet. In this work, the performance of different sub-grid scale (SGS) models of large-eddy simulation (LES) is investigated against their capability to describe the separation bubble of a blunt plate under a turbulent inlet. This is aimed at starting a broader research on the actual role of turbulence on the aerodynamic behaviour. Together with the Smagorinsky, the dynamic and the WALE SGS models, also the URANS k-ε and k-ω SST have been compared. The results show that whether URANS is able to accurately describe the undisturbed case, it gives a wrong turbulent inlet in the other one. Although the LES technique can improve the accuracy of this complex configuration, the choice of a suitable averaging time strongly affects the validation of the model. It was found that the role of the SGS eddies is not preponderant. Then a complex system of equations may lead to instability of the solver and prohibitive time step requirements. Among the SGS models investigated, the Smagorinsky SGS model, using a damping function to tackle the near-wall behaviour, qualifies then as a good candidate for further, more complex, geometries

1   Introduction

In the assessment of the aerodynamic loads for a variety of bluff bodies in the Atmospheric Boundary Layer (ABL), the common practice advices not to take into account Free Stream Turbulence (FST) as an essential parameter (Simiu & Scanlan, 1986). This assumption, is based on the interpretation of the role of the length scale of turbulence on the aerodynamics. In fact, the integral length scale of turbulence is usually much larger than the height of the boundary layer of the object of interest. It is then acceptable to consider turbulence as a slow fluctuation of the mean velocity, which does not modify the flow pattern (Buresti, 2012). Miley (Miley, 1982) pointed out that the boundary layer of an aerofoil is only sensitive to the turbulent fluctuations on the order of the size of the aerofoil boundary layer itself. The FST has an effect on the unsteady variation of the real angle of attack, which can be well neglected in experiments and simulations. Simms (Simms, Schreck, Hand, & Fingersh, 2001) further stresses Miley's discussion, adding that as the small scales carry a least quantity of energy, they do not affect the performance of an aerofoil. Therefore, inflow turbulence can be well neglected, as it was done for the famous NREL Ames Wind Turbine (Hand, Simms, & Fingersh, 2001).

Nonetheless, the interaction of bluff bodies and FST represent a niche of the research. It was found that FST acts differently with boundary (BL) and shear layers (SL). Three basic mechanisms have been conjectured. Turbulence i) promotes the transition to turbulence for BL and SL, ii) enhances the mixing of SL and the entrainment of turbulence in the near wake, and iii) is itself distorted by the mean-flow past the bluff body (Zdravkovich, 1997). However, it is unclear which turbulence statistics are suitable for the understanding of such a complex interaction. A thorough discussion on these aspects was provided by Bearman and Morel (Bearman & Morel, 1983), but an elucidative answer is still awaited. As a conclusive statement, the effect of the largest scales of turbulence seems to be weaker than that of the smaller scales (Bearman, 2006; Nakamura & Ohya, 2006). Investigation of the

mutual relationship between the integral length scale and the turbulent intensity may enhance understanding the role of large turbulence integral length scales and boundary layer, particularly for ABL flows.

The work of this paper represents a preliminary step of a broader research on Urban Wind Energy and the role turbulence plays in affecting Wind Turbine Aerodynamics, with specific reference to two major issues: i) the effect that turbulence has on the overall aerodynamic behaviour and performance and ii) the signature turbulence, which acts as inlet turbulence. The aim of this work is to assess the performance of Computational Fluid Dynamics (CFD) in predicting the evolution of a separation bubble, which occurs on the simplified geometry of a blunt plate under both turbulent and undisturbed inlet conditions. In particular, several turbulence modelling techniques are compared, with a particular discussion on the role of sub-grid scale (SGS) models in Large Eddy Simulations (LES). A comparison with URANS technique is also provided to be thorough. The obtained results are aimed at defining an LES framework to be employed in further simulations.

2   Experimental Results

This investigation replicates numerically the experimental setup of Sasaki and Kiya (Kiya & Sasaki, 1985; Sasaki & Kiya, 1983, 1985). The experiment consisted of a blunt flat plate, BP, with right angled corners, whose sides are aligned to the in-flow, and of such a length that the interaction between the leading and the trailing edge is prohibited (Fig. 1a).
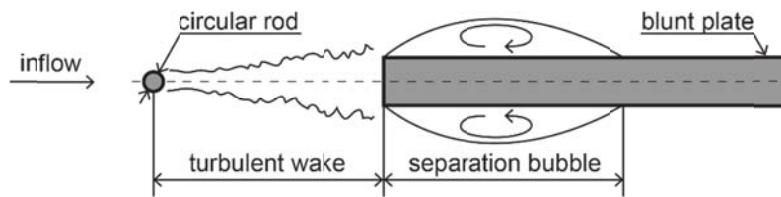

Figure 1. Blunt plate experiment set, with flow configuration, after (Sasaki & Kiya, 1985).

A set of upstream circular cylindrical rods have been used to simulate different turbulent inlets (Tab. 1).

Table 1. Normalised turbulence properties at the leading edge.

Configuration		Turbulence statistics	
d [mm]	l [mm]	$I_u = \sqrt{\overline{u'^2}}/\bar{u}$ [%]	x_R/H [-]
5.0	100	6.9	2.9
3.0	180	3.7	5.9
undisturbed		1.2	9.5

In this work, only the undisturbed and the 5-100 couplet are considered. The inlet velocity upstream to the generator of turbulence was kept uniform and constant at a value of $u_\infty = 20\,m/s$. This yields a Reynolds number $Re = u_\infty(2H)/v$ of 2.6×10^4 throughout the experiment. Half the height of the blunt plate is $H = 1.0\,cm$. This height is taken as the reference length. The inlet turbulence statistics, as reported in Tab. 1, were measured at the reference position $(x/H = 0, y/H = 0.1)$. A constant temperature hot-wire anemometer with an I-probe was used to measure the mean and fluctuating component of velocity, while a strain gauge transducer provided the plate pressure fluctuations. The experiment shows a strong correlation of FST and the statistics of the reattachment. The simplicity of the experiment is interesting for assessing the methodology to be used in further studies on the actual flow pattern.

3   Methodology

3.1   Large Eddy simulation and Sub-Grid Scale modelling

In this work different turbulence modelling techniques are investigated. Both the URANS and the Large Eddy Simulation (LES) were implemented. In LES, the sub-grid scale (SGS) eddies are modelled, using the definition of an eddy viscosity v_{sgs} to simulate their influence with the larger scales. Among the various SGS models, the classic Smagorinsky approach (Lilly, 1966) was chosen, together with the dynamic Germano (Germano, Piomelli, Moin, & Cabot, 1991; Lilly, 1992) and the Wall Adapting Local Eddy-viscosity (WALE) (Nicoud & Ducros, 1999) model for comparison.

The Smagorinsky-Lilly SGS model, as implemented in openFoam, assumes that a kinematic sub-grid scale viscosity v_{sgs} can be defined such that the residual stress tensor τ_{ij} is proportional to the strain rate S_{ij} of the resolved flow (like the Boussinesq assumption for RANS). Therefore, τ_{ij} can be written:

$$\tau_{ij} = -2\rho v_{sgs} \widetilde{S_{ij}} + \frac{1}{3} R_{ii}\delta_{ij} = -\rho v_{sgs}\left(\frac{\partial \widetilde{u}_i}{\partial x_j} + \frac{\partial \widetilde{u}_j}{\partial x_i}\right) + \frac{1}{3}\tau_{ii}\delta_{ij} \tag{1}$$

where indicates the filtering operation and v_{sgs} is defined, up to a constant, as (Pope, 2000):

$$v_{sgs} = \left(C_{sgs}\Delta\right)^2 |\widetilde{S}| = \left(C_{sgs}\Delta\right)^2 \sqrt{2\widetilde{S_{ij}S_{ij}}} \quad \text{with} \quad C_{sgs} = 0.17 \tag{2}$$

This formulation leads to an unphysical behaviour near the wall. To overcome this issue, a damping function, such as the van Driest approach (Van Driest, 1956), is used:

$$l_{sgs} = C_{sgs}\Delta\left(1 - e^{-y^+/A^+}\right) \quad \text{with} \quad A^+ = 26 \tag{3}$$

The Germano model remedies the limitation of a constant model coefficient by filtering a second time the SGS stresses. This approach provides a dynamic calculation of the model constant. The Germano identity (4) relates the Leonardt stresses L_{ij} to the sub-test T_{ij} and the sub-grid stresses τ_{ij};

$$L_{ij} = \widetilde{\overline{u_i}\,\overline{u_j}} - \widetilde{\overline{u}}_i\widetilde{\overline{u}}_j = T_{ij} - \widetilde{\tau}_{ij}; \quad T_{ij} = \widetilde{\overline{u_iu_j}} - \widetilde{\overline{u}}_i\widetilde{\overline{u}}_j; \tag{4}$$

The SGS stresses are then formulated using the definition of SGS viscosity following eq. (2). Substituting with eq. (4), the asymmetric part of the SGS stresses is found:

$$M_{ij} = T_{ij} - \frac{1}{3}T_{kk}\delta_{ij} = -2C_s\widetilde{\Delta}^2\left|\widetilde{\overline{S}}\right|\widetilde{\overline{S}}_{ij}; \quad m_{ij} = \tau_{ij} - \frac{1}{3}\tau_{kk}\delta_{ij} = -2C_s\overline{\Delta}^2|\overline{S}|\overline{S}_{ij}; \quad L_{ij}^a = L_{ij} - \frac{1}{3}L_{kk}\delta_{ij} = M_{ij} - \widetilde{m_{ij}} \tag{5}$$

The dynamic constant C_s can be evaluated by contracting eq. (5).

$$C_s = \frac{1}{2}\left(\frac{L_{ij}\overline{S}_{ij}}{M_{ij}\overline{S}_{ij}}\right) \tag{6}$$

In the present work an evaluation of C_s based on the minimisation of the error e_{ij} related to the Leonardt stresses, as proposed by Lilly, was used:

$$\frac{\partial e_{ij}}{\partial C_s} = 0; \quad \frac{\partial^2 e_{ij}}{\partial C_s^2} > 0; \quad C_s = \frac{1}{2}\left(\frac{L_{ij}M_{ij}}{M_{ij}^2}\right) \tag{7}$$

The WALE model is an algebraic model of the Smagorinsky family, overcoming the major drawbacks of the method that are the lack of an effect due to the vorticity of the SGS, i.e. the deviatoric part of τ_{ij}, and the following incorrect near-wall behaviour. The model is based on the

choice of a suitable spatial operator that respects some mathematical constraints and is based on the traceless symmetric part of the strain tensor $|\tilde{S}|$. The eddy viscosity associated with the model reads:

$$v_{sgs}=(C_w\varDelta)^2\,\frac{\left(S_{ij}^d S_{ij}^d\right)^{3/2}}{\left(\bar{S}_{ij}\bar{S}_{ij}\right)^{5/2}+\left(S_{ij}^d S_{ij}^d\right)^{5/4}}\quad\text{with}\quad C_w=0.5 \tag{8}$$

The formulation of the model itself allows for a more stable computation and an increased accuracy of the near-wall behaviour, which in turn gives a lessen requirement of the near-wall mesh. Moreover, this is well-suited for complex geometries as it is only computed locally without any dynamic adjustment.

4   Numerical details

To investigate the effect of various SGS models, a series of simulations have been made, in order to gain confidence with every computational technique. The various simulations are stated in Table 1. Two geometries have been modelled, based on the desired turbulence at the inlet. The turbulent inflow case reproduces the couplet *d-l=5-100* of the experimental setup, described in Section 2. The smooth inflow case is the undisturbed condition subject to a constant inlet velocity of *20 m/s*. Using the available computational sources of the computational cluster BlueBEAR at the University of Birmingham, both openFoam v.3.0.1 (3D simulations) and Ansys CFX v.16.2 (2D simulations) have been used.

Table 2. List of simulations and software used.

Computational models		
Turbulence models	2D model	
	Turbulent inflow	Smooth inflow
1 URANS *k-ε*	CFX	CFX
2 URANS *k-ω* SST	CFX	CFX
3 LES Smagorinsky	CFX	CFX
4 LES Dynamic Germano	CFX	CFX
5 LES WALE	CFX	CFX
	3D model	
6 LES Smagorinsky	openFoam	openFoam

In order to set up the model, the meshing strategy was chosen: a set of four grids have been implemented. The 3D simulations rely on a structured grid at an earlier stage of the research, therefore the $y^+\approx1$ requirement is not respected for the 3D results. The grids show the following number of elements:

- Smooth inlet C-grid *2,858,700* hexahedrical elements with 27 blocks;
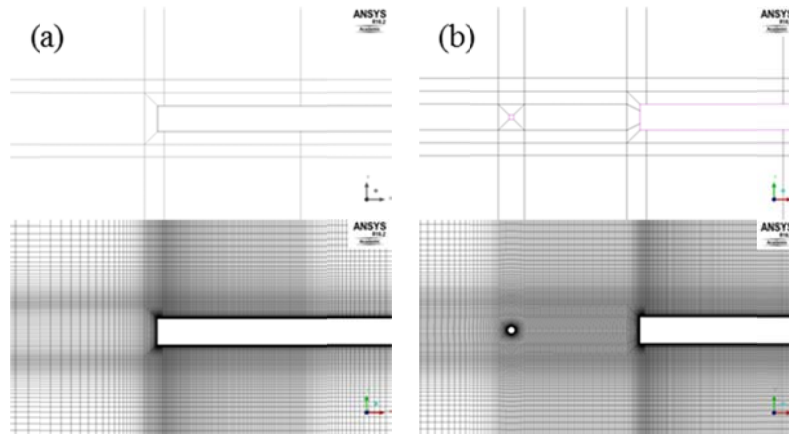- Turbulent inlet O-grid/C-grid *7,681,000* hexahedrical elements with 25 blocks.

Figure 2. Computational structured grid: (a) smooth and (b) turbulent inlet case, with blocking strategy.

In order to fine-tune the mesh, an additional set of 2D grids has been developed to study the variation of y^+ and the requested number of elements. An H-grid approach was hence compared to an O-grid/C-grid one. It resulted that if an analogous near-wall spacing is kept, the use of a C-grid is much more economical (*51,261* el.) than an H-grid (*70,566* el.). However, the latter presents a reduced skewness, which is important for a stable simulation. An H-grid is then implemented, with an extra optimisation of the near-wall blocking strategy. The following mesh has resulted:
-   Smooth inlet H-grid *42,114* hexahedrical elements with 24 blocks (Fig.2a);
-   Turbulent inlet C-grid/Hgrid *57,622* hexahedrical elements with 45 blocking (Fig.2b).
The instantaneous value of y^+ is shown in Fig. 3 for both the 3D- and the 2D-meshes. This givea a parameter to better interpret the results, which follow in Section 5.
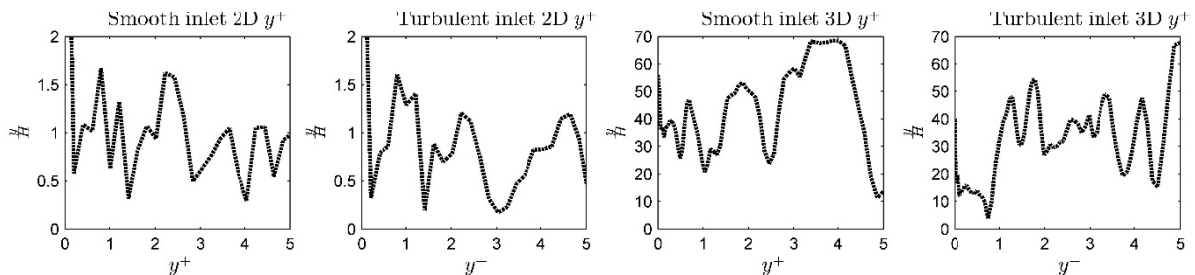

Figure 3. y^+ instantaneous value for the 2D model with (a) smooth and (b) turbulent inlet, and for the 3D models with (c) smooth and (d) turbulent inlet.

The solver was initialised using the potential flow. As regards the boundary conditions, a constant inlet for the velocity has been set while a neutral pressure condition was posed at the outlet. The 3D model uses an outlet condition which is able to turn the Leibniz or the Neumann condition depending on the direction of the flow, to tackle such a turbulent outlet. The time step was chosen in order to yield a stable accurate simulation and to limit the value of the Courant number. Following values have been imposed:
-   3D simulation, 1e-05 for all the models;
-   2D simulation, *k-ε 1e-02, k-ω 1e-04*, LES *2.5e-05*.
In order to get a well-developed flow, the simulations have been run for at least *3s* with an additional averaging time for the LES simulations of at least *1.5s*.

5   Results and discussion

In this Section, the choice strategy for the turbulence model to be implemented for further investigations on similar flow patterns is discussed. The results compare the URANS strategy against

different LES SGS models, with an assessment on the behaviour of 2D and 3D models. A twofold problem is noticeable. The model to be effective should be accurate in modelling both the reattachment length and the turbulence at the inlet, therefore a steep difference in the performance of various models is expected in the undisturbed or turbulent inlet cases. An inaccurate reattachment length is not easily attributable to the accuracy of the model itself, as the turbulence at the inlet depends on the way the model tackles the wake originating from the upstream cylinder and the relative turbulence intensity and length scale.

Another important issue is the averaging of the instantaneous quantities over a significantly long time. Strictly, it should not be possible to compare statistics with different averaging time. While URANS provides an already averaged solution, LES relies on a suitable averaging of the instantaneous quantities to draw conclusions on the final results. A possible mismatch in the results, might be largely due to the choice of the averaging time. However, the choice of the actual averaging time is based on the computational costs, posing a challenging validation with available experimental results.

5.1 Velocity results

The results for the mean velocity $\bar{u}/u_\infty$ and the turbulence intensity $\sqrt{\overline{u'^2}}/\bar{u}$ are reported for the undisturbed (Fig.4) and the turbulent inlet (Fig.5), for every turbulence model proposed.

As regards the undisturbed case (Fig. 4), the URANS technique shows a good performance. Although the k-ε model fails in describing the trend of the fluctuating component, the k-ω SST model correctly reproduces the turbulence at the inlet, but it overestimates the height of the separation bubble.

For the LES technique, the 3D Smagorinsky model is effective in describing both the mean and fluctuating component of the velocity. The mismatch in the mean component is owed to an error in the turbulence intensity at the inlet. This is due to numerical diffusion issues, caused by the skewness of the C-Grid mesh implemented. It is also clear that a better averaging is needed, as the trend in the curves is still affected by the instantaneous oscillations. If the 3D LES model is able, to some extent, to accurately reproduce the turbulence at the inlet, among the different SGS models, the Smagorinsky one is generally much more performant than the more complex Dynamic and WALE model, if the Van Driest damping function is used near the wall, as the results provided are closer to the experimental ones.
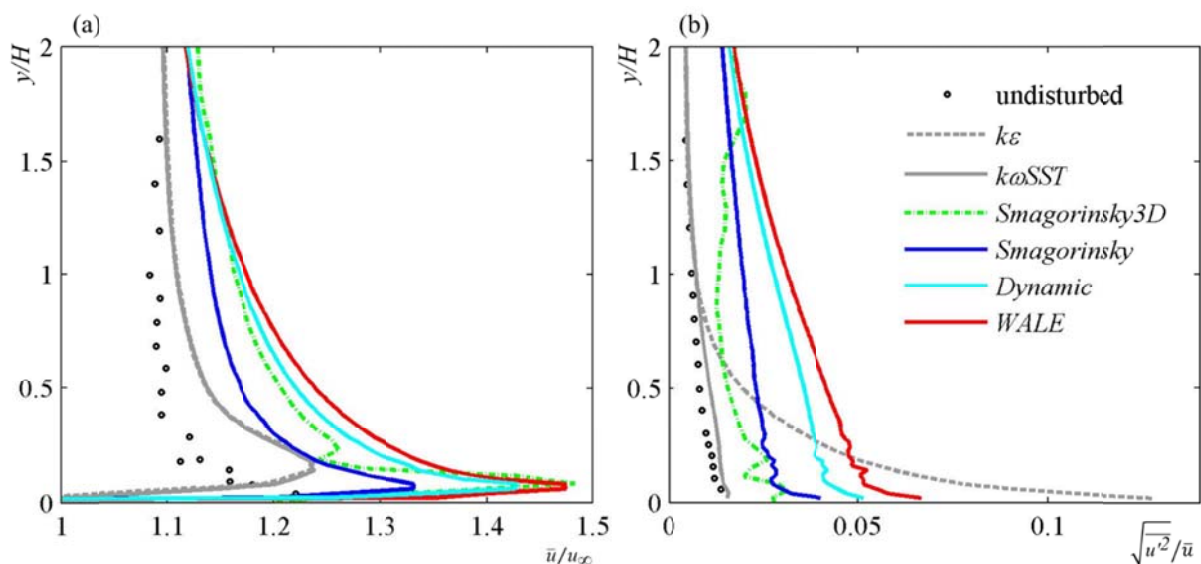

Figure 4. Undisturbed inlet case: (a) mean velocity and (b) turbulence intensity

As regards the modelling of the turbulent inlet configuration (Fig. 5), the sparsity of the results shows the evident complexity of the problem. In particular, two issues unfold: the modelling of the actual turbulent inlet, which essentially depends on the accurate modelling of the wake and its decay, and the

accurate prediction of the reattachment length onto the plate. Hence, a mismatch in the reattachment length may also depend on a wrong turbulent inlet. Fig. 5 shows that LES is absolutely able to provide the correct trend of both the mean and fluctuating component of velocity. A further simulation, Smagorinsky3D2, is proposed for completeness with a reduced averaging time and a refined mesh: the role of the average is preponderant. As the 2D models show an obvious difficulty in being physically sound, it is difficult to state here their performance. Within URANS technique, the k-ε model yields unphysical results, while the k-ω SST model, although it dampens turbulence because of its lower diffusivity, provides a reduced mismatch than 2D LES models.
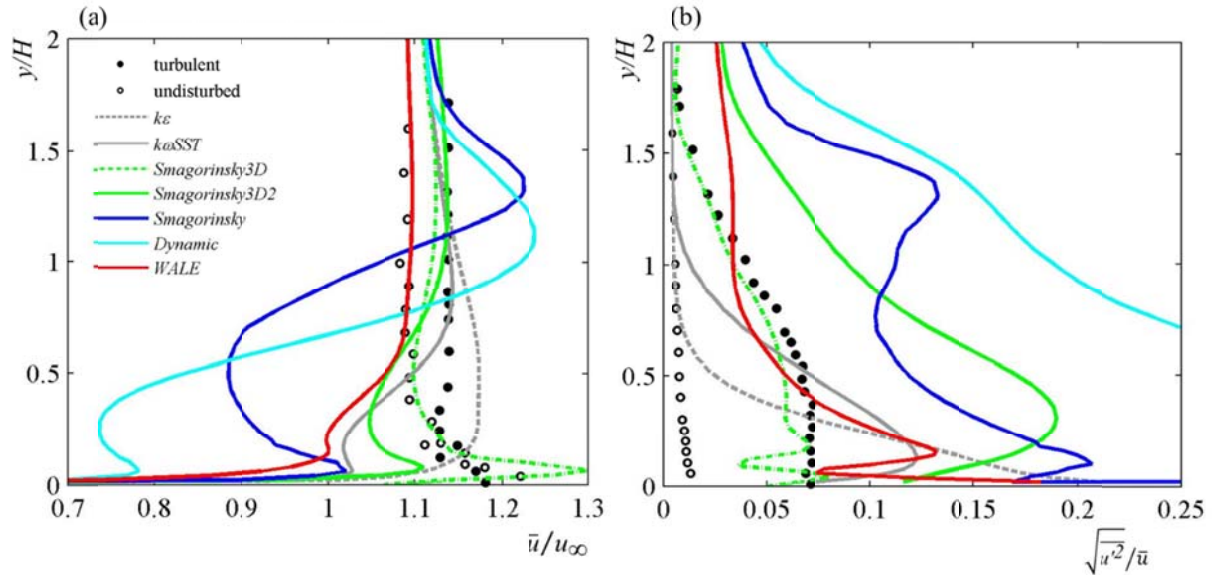

Figure 5. Turbulent inlet case: (a) mean velocity and (b)turbulence intensity

In order to draw exhaustive conclusions, other parameters need to be assessed and compared.

5.2   Pressure results

The pressure coefficient $c_p = \sqrt{\overline{p'^2}} / (1/2\rho\bar{u}^2)$ for the undisturbed (Fig. 6a) and turbulent (Fig. 6b) inlet case is shown. While the 3D model provides good performance in the turbulent case (but showing that a better refinement of the mesh is needed), it yields unphysical results for the undisturbed case. This is due to the numerical diffusion which modifies the actual turbulence at the inlet of the plate. The URANS technique shows here the best performance, although the near edge behaviour is not reproduced by the k-ω SST. Among the SGS models, the Smagorinsky model shows a better performance, as the minimum of the pressure coefficient trend is diverted downstream towards the experimental result.
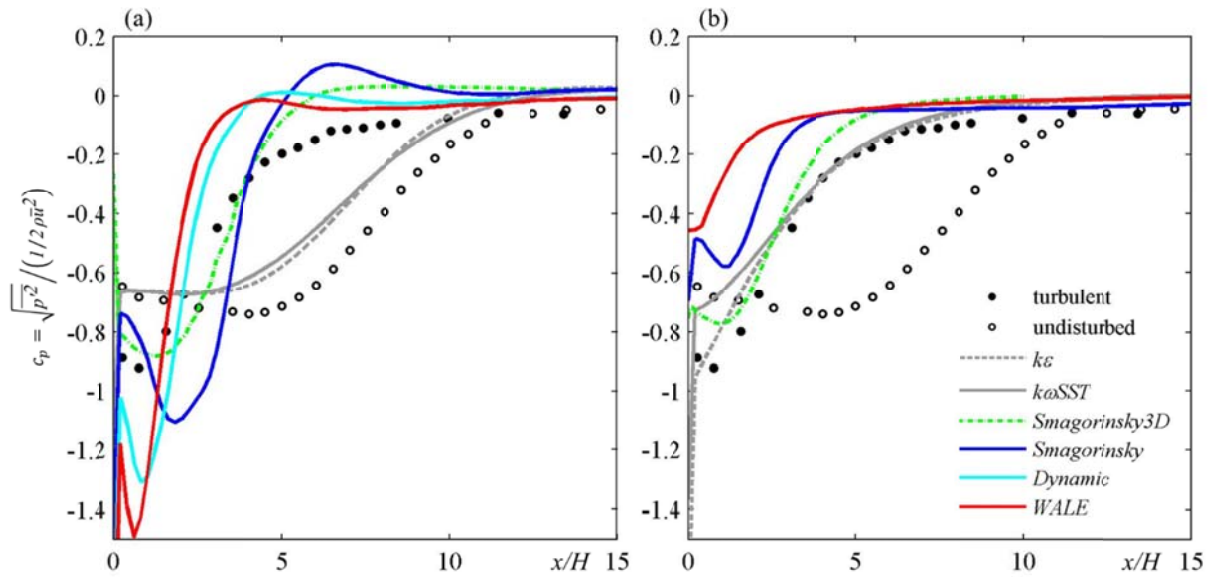
Figure 6. Surface pressure distribution for the (a) undisturbed and the (b) turbulent case.

5.3 Reattachment length and separation bubble

A more immediate comparison with the experiment can be done plotting the reattachment lengths. As regards the undisturbed case, the URANS technique shows the best behaviour, as expected from the results for pressure and velocity and the diffusion which occurs in the 3D LES model. The turbulent inlet case shows a good behaviour of the 3D LES model, however the reattachment length is delayed. This is due to the mesh refinement, which needs fine-tuning. The URANS technique is not able to model the correct reattachment length. As regards the SGS models, the Smagorinsky with Van Driest damping shows the best performance, as the trend of the phenomenon is correctly catched.
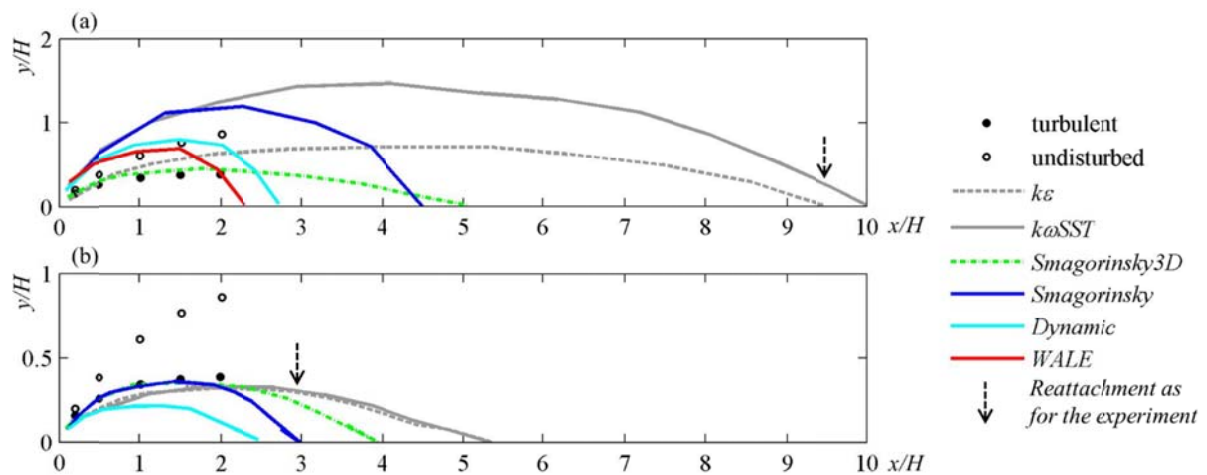

Figure 7. Centreline of separated shear layer for (a) undisturbed and (b) turbulent case.

5.4 Instantaneous flow pattern

In closing, a flow visualisation plot can clarify the numerical results previously presented and discussed. A comparison between the different SGS models is provided (Fig. 8). The distinctive 2D turbulence features are recognisable. The Dynamic and WALE SGS models show in general a more diffusive behaviour, with smearing of the velocity field. Nonetheless, the behaviour of the SGS models confirms that the effect of SGS eddies is marginally influencing the result, while complicating equations introducing possible instability prevents the practical usage of the models.
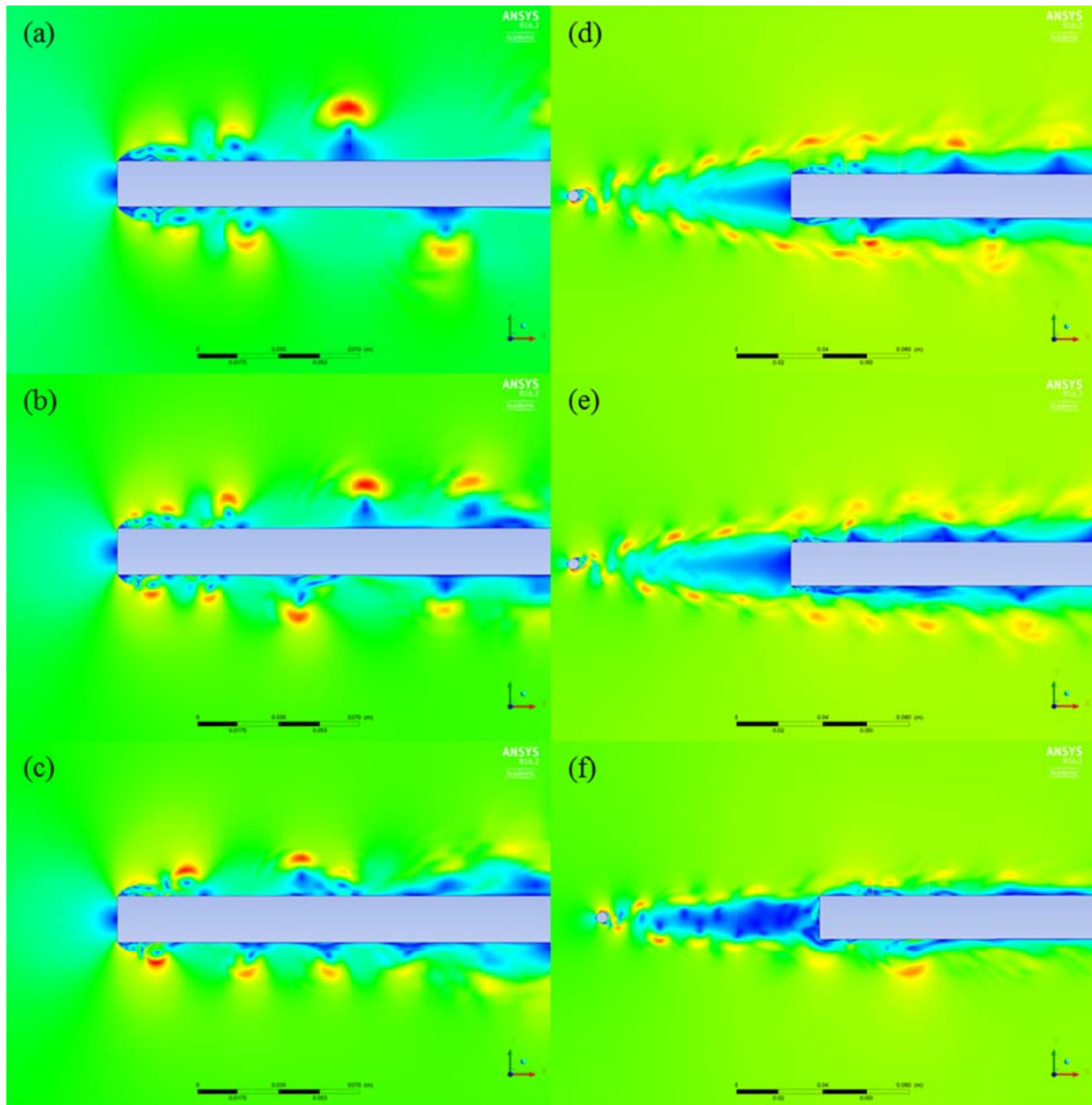
Figure 8. Flow pattern of instantaneous velocity magnitude for (a,d) Smagorinsky, (b,e) Dynamic and (c,f) WALE SGS model for the undisturbed (a,b,c) and the turbulent (d,e,f) case.

In Fig. 9 the averaged results of the URANS models show that turbulence in the wake of the rod is immediately dissipated, while for the undisturbed case the results are almost overlapping.

In Fig. 10 the instantaneous flow pattern relevant to the 3D models confirms the role played by the cross-dimension. It also shows the diffusive numerical turbulence, which affects the results and is only removable by further fine-tuning the mesh. It is also noticeable the accuracy in the modelling of the wake which feeds energy in the separation bubble, anticipating its reattachment.
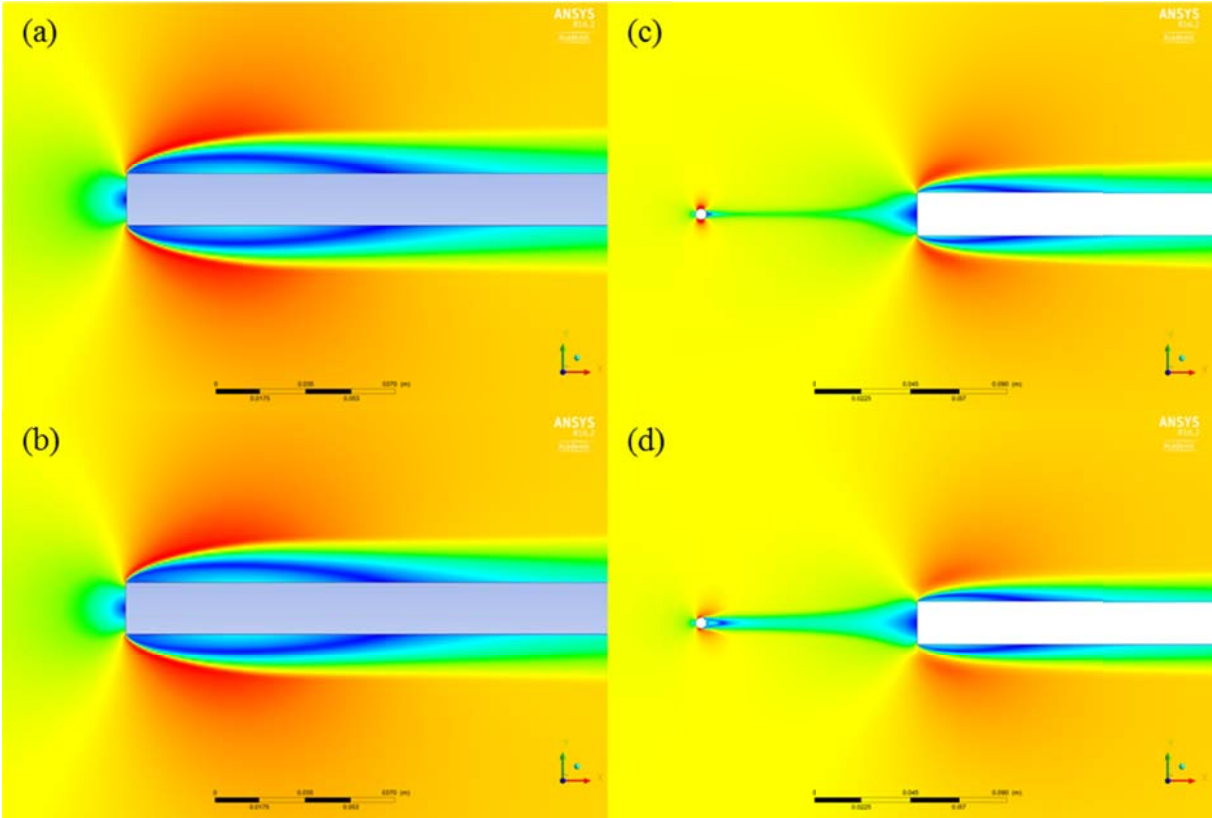
Figure 9. Averaged flow field for the URANS *k-ε* (a,c) and *k-ω SST* (b,d) undisturbed (a,b) and turbulent (d,e) case.
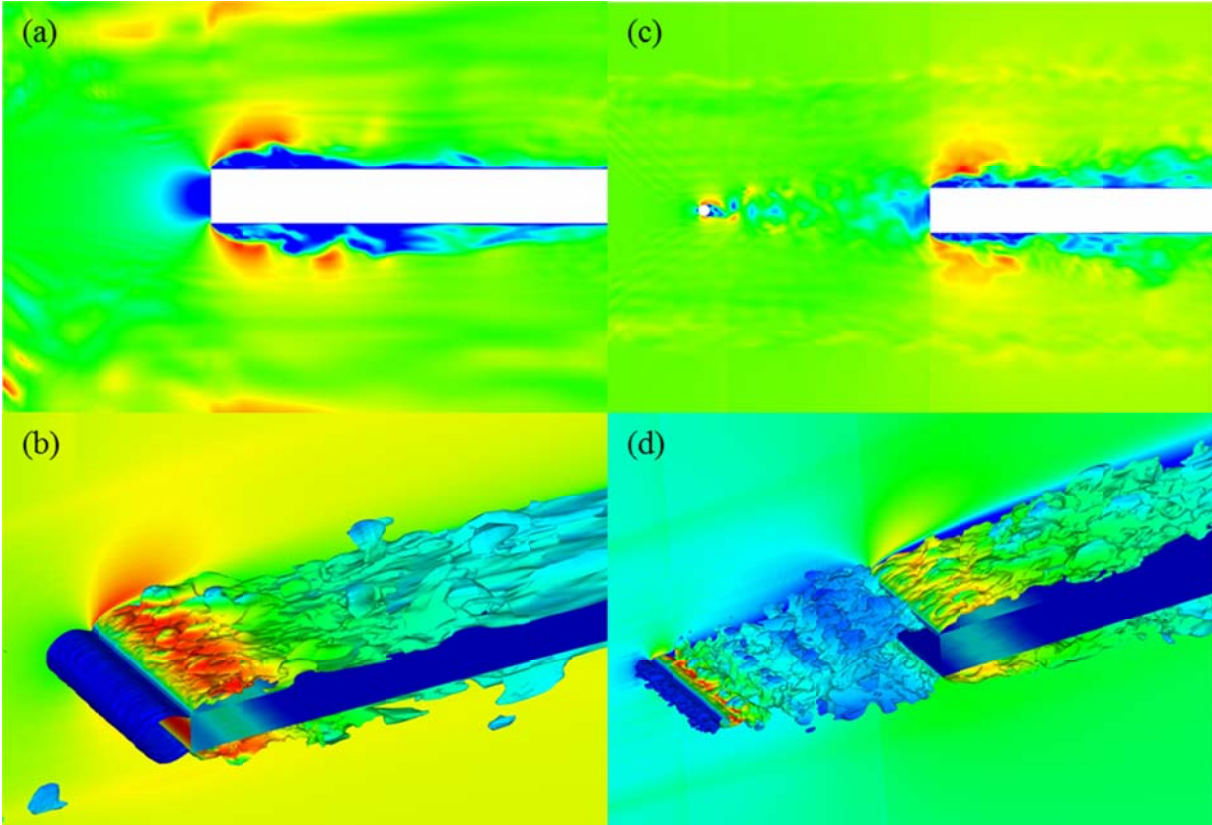

Figure 10. Instantaneous velocity flow pattern for the Smagorinsky 3D model (a) undisturbed and (c) turbulent case, and isocontour of velocity visualisation (b,d).

6   Conclusions, recommendations and further steps of research

In this preliminary work different turbulence modelling techniques have been assessed in their performance in modelling the separation bubble of a blunt flat plate, which occurs under a turbulent inlet. The comparison has focused in particular on different SGS models within the LES technique. It has been found that the Smagorinsky model is the most performant method, as the results are closer to the experimental ones, once agreed upon the correct refinement of the near-wall mesh, the use of a suitable damping function, and the proper choice of the time-step and averaging time, which takes into account computational costs and stability issues. The role of the SGS eddies is nevertheless not as important as that of the mesh, as it is shown by the 3D simulation and its accuracy. It is though unclear whether these conclusions can be stated in general for a set of 3D models.
This could represent a further step in the research of the role of SGS modelling in LES.

7   Acknowledgements

8   References

Bearman, P. W. (2006). An investigation of the forces on flat plates normal to a turbulent flow. *Journal of Fluid Mechanics*, *46*(1), 177.

Bearman, P. W., & Morel, T. (1983). Effect of free stream turbulence on the flow around bluff bodies. *Progress in Aerospace Sciences*, *20*(2–3), 97–123.

Buresti, G. (2012). *Elements of Fluid Dynamics*. London: Imperial College Press.

Germano, M., Piomelli, U., Moin, P., & Cabot, W. H. (1991). A dynamic subgrid-scale eddy viscosity model. *Phys. Fluids A Fluid Dyn.*, *3*(7), 1760.

Hand, M., Simms, D., & Fingersh, L. (2001). Unsteady aerodynamics experiment phase VI: wind tunnel test configurations and available data campaigns.

Kiya, M., & Sasaki, K. (1985). Structure of a turbulent separation bubble. *Journal of Fluid Mechanics*, *137*(1), 83.

Lilly, D. K. (1966). On the application of the eddy viscosity concept in the inertial sub-range of turbulence. *NCAR Manuscript, No. 123*(January), 1–19.

Lilly, D. K. (1992). A proposed modification of the Germano subgrid-scale closure method. *Physics of Fluids A: Fluid Dynamics*, *4*(3), 633.

Miley, S. (1982). A catalog of low Reynolds number airfoil data for wind turbine applications. Retrieved from http://wind.nrel.gov/public/library/3387.pdf

Nakamura, Y., & Ohya, Y. (2006). The effects of turbulence on the mean flow past square rods. *Journal of Fluid Mechanics*, *137*(1), 331.

Nicoud, F., & Ducros, F. (1999). Subgrid-scale stress modelling based on the square of the velocity gradient tensor. *Flow, Turbulence and Combustion*, *62*(3), 183–200.

Pope, S. B. (2000). *Turbulent Flows*. *Book* (Vol. 1).

Sasaki, K., & Kiya, M. (1983). Free-stream turbulence effects on a separation bubble. *Journal of Wind Engineering and Industrial Aerodynamics*, *14*(1–3), 375–386.

Sasaki, K., & Kiya, M. (1985). Effect of Free-Stream Turbulence on Turbulent Properties of a Separation-Reattachment Flow. *Bulletin of JSME*, *28*(238), 610–616.

Simiu, E., & Scanlan, R. H. (1986). *Wind Effects on Structures: An Introduction to Wind Engineering* (Wiley). New York.

Simms, D., Schreck, S., Hand, M., & Fingersh, L. (2001). NREL unsteady aerodynamics experiment in the NASA-Ames wind tunnel: a comparison of predictions to measurements.

Van Driest, E. R. (1956). On Turbulent Flow Near a Wall. *Journal of the Aeronautical Sciences*, *23*(11), 1007–1011.

Zdravkovich, M. M. (1997). *Flow Around Circular Cylinders*. *Flow around circular cylinders*.